CHEMMEDCHEM

DOI: 10.1002/cmdc.200700325

Synthesis and Biological Activity of a Novel Inhibitor of Dihydroceramide Desaturase

Jose M. Munoz-Olaya,[a] Xavier Matabosch,[a] Carmen Bedia,[a] Meritxell Egido-Gabás,[a] Josefina Casas,[a] Amadeu Llebaria,[a] Antonio Delgado,[a, b] and Gemma Fabriàs*[a]

A novel mechanism-based dihydroceramide desaturase inhibitor (XM462) in which the substrate C5 methylene group is replaced by a sulfur atom is reported. Dihydroceramide desaturase inhibition occurred both in vitro and in cultured cells with IC_{50} values of 8.2 and 0.78 μM, respectively, at a substrate concentration of 10 μM. In vitro experiments showed that XM462 produced a mixed-type inhibition ($K_i = 2$ μM, $\alpha = 0.83$). LC-MS analyses showed that accumulation of endogenous dihydroceramides occurred in cells upon treatment with XM462 in serum-free medium, whereas ceramides built up in controls. In addition, XM462 was found to be metabolised to its 1-glucosyl and 1-phosphocholine derivatives, and to the products of N-deacylation and reacylation with palmitoyl and stearoyl groups. In Jurkat A3 cells cultured in serum-free medium, viability, as the percentage of trypan blue unstained cells in total cells, was reduced upon XM462 treatment (5 μM, 24 h), but not in controls. The interest of this compound is discussed.

Introduction

Ceramide is involved as a mediator of apoptosis induced by a variety of signalling molecules or stress events, which lead to a transient intracellular increase of this bioactive lipid. In general, the induced ceramide rise results from activation of sphingomyelinases or de novo biosynthesis. In the de novo pathway, ceramide is biosynthesized from L-serine in four distinct steps, the last one being the Δ^4-desaturation of dihydroceramide to ceramide by dihydroceramide desaturase. This protein is coded by the human Des1 gene.[1,2] Human Des1 exhibits high dihydroceramide Δ^4desaturase and very low C4 hydroxylase activities, whereas Des2, another homologue identified in mouse and human, exhibits bifunctional sphingolipid C4 hydroxylase and Δ^4desaturase activities.[3] The Des2 protein, which is preferentially expressed in small intestinal cells, is probably responsible for the biosynthesis of enriched glycophytosphingolipids in that tissue.[4,5]

Dihydroceramides have been regarded as innocuous lipids for years.[6] This assumption was sustained by the failure of exogenous dihydroceramides with short *N*-acyl chains to mimic the antimitogenic effects caused by the respective ceramides in cultured cells.[6–8] However, recent reports[9–11] indicate that dihydroceramides are in fact bioactive lipids, although their effect may differ from those elicited by ceramides. The use of biophysical models,[10] as well as genetic[9] and pharmacological[9,11,12] tools to decrease dihydroceramide desaturase activity has proven crucial to reveal the biological activity of dihydroceramide derivatives. Some of these pharmacological tools comprise fenretinide,[9,11] γ-tocopherol,[12] and GT11.[13]

The design, synthesis, and dihydroceramide desaturase inhibitory activity of the cyclopropene ceramide GT11 was first reported in 2001.[13] Further studies showed that GT11 was a competitive inhibitor ($K_i = 6$ μM)[14] and identified the structural requirements for inhibitory activity, which included the presence of the cyclopropene ring in place of the ceramide double bond, the natural 2*S*,3*R* stereochemistry, a free hydroxyl group at C1, and the amide function, although certain surrogates thereof are also active.[14,15] GT11 was also found to inhibit dihydroceramide desaturase in cultured cells.[16]

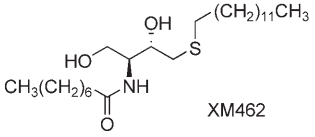

XM462

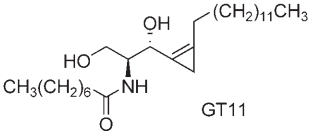

GT11

The approach previously followed in the design of GT11 was applied to obtain a new dihydroceramide desaturase inhibitor, named XM462. With this rationale, the mechanistic aspects of enzymatic desaturation together with the reported structural features of known fatty acyl-CoA desaturase inhibitors were taken into account. The design, synthesis, and biological activity of this compound both in vitro and in Jurkat A3 human leukaemia cells are reported in this article.

[a] *J. M. Munoz-Olaya, Dr. X. Matabosch, Dr. C. Bedia, Dr. M. Egido-Gabás, Dr. J. Casas, Dr. A. Llebaria, Dr. A. Delgado, Dr. G. Fabriàs*
Research Unit on BioActive Molecules
Departamento de Química Orgánica Biológica
Instituto de Investigaciones Químicas y Ambientales de Barcelona, CSIC
Jordi Girona 18, 08034 Barcelona (Spain)
Fax: (+34) 93-204-5904
E-mail: gfdqob@cid.csic.es

[b] *Dr. A. Delgado*
Unidad de Química Farmacéutica (Unidad Asociada al CSIC)
Facultad de Farmacia
Universidad de Barcelona
Avda. Juan XXIII s/n, 08028 Barcelona (Spain)

Results

Synthesis of XM462

Synthesis of XM462 was accomplished as depicted in Scheme 1 from epoxide **1**, easily available from Garner aldehyde following described protocols.[17] Nucleophilic opening of

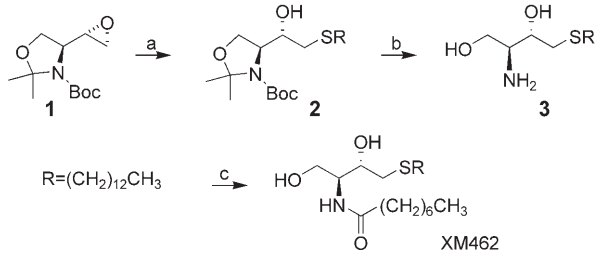

Scheme 1. Synthesis of XM462. Reagents and conditions: a) $C_{13}H_{27}SH$, NaH, DMF, 40 °C; b) TFA, CH_2Cl_2; c) $C_7H_{15}COCl$, 50% NaOAc/H_2O, THF.

1 with *n*-tridecylthiolate, followed by simultaneous removal of the *O*,*N*-acetal and Boc groups and final selective *N*-acylation with octanoyl chloride under Schotten-Bauman conditions (THF, 50% aq. NaOAc) afforded target XM462 in 80% overall yield.

Desaturation of DHCerC6NBD

The finding that 6-[*N*-(7-nitro-2,1,3-benzoxadiazol-4-yl)amino] hexanoylsphinganine (DHCerC6NBD) is desaturated to the ceramide analogue in several cell lines[18] prompted us to use this compound as substrate to measure dihydroceramide desaturase activity in vitro for further inhibition studies. Desaturation of DHCerC6NBD was evaluated in rat liver microsomes and Jurkat human leukaemia cells. Liver contains almost exclusively Des1[4] and LC-MS analysis of the Jurkat cells sphingolipidome revealed the presence of only trace amounts of phytosphingolipids, in contrast to large quantities of sphingo- and dihydrosphingolipids (data not shown). Therefore, although conclusive genetic evidence has not been obtained, the sphingolipid profile highly supports that Des1 is the predominant dihydroceramide desaturase in this cell model.

To determine the kinetic parameters of DHCerC6NBD desaturation, rat liver microsomes were incubated for one hour with different substrate concentrations between one and 40 μM and lipids were then analysed by HPLC with a fluorimetric detector (HPLC-FD). The identity of both substrate and product was confirmed with synthetic standards and LC-MS. These experiments showed that DHCerC6NBD was desaturated to 6-[*N*-(7-nitro-2,1,3-benzoxadiazol-4-yl)amino] hexanoylsphingosine (CerC6NBD) with a K_m of 7.7 μM and a V_{max} of 19.3 pmol h^{-1} mg^{-1}.

The desaturation of DHCerC6NBD in Jurkat human leukaemia cells was also investigated by incubation with the substrate (10 μM) under the conditions described in the experimental section and further HPLC-FD analysis of both media and cell lysates. The two types of samples contained the same species in similar ratios, but the absolute amounts were higher in the media (data not shown). Therefore, only the medium was analysed in further experiments, which showed the presence of both DHCerC6NBD and CerC6NBD, and the 1-phosphate, 1-glucosyl and 1-phosphocholine derivatives of DHCerC6NBD (Figure 1). The identity of all these metabolites was confirmed by LC-MS (data not shown).

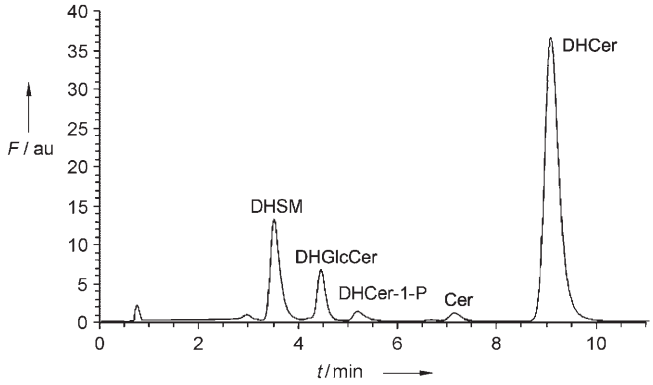

Figure 1. HPLC-FD profile of fluorescent sphingolipids produced from DHCerC6NBD in Jurkat A3 cells. Approximately 4×10^5 Jurkat A3 cells were incubated with 10 μM DHCerC6NBD (4 °C for 30 min and then 37 °C for 24 h after media renewal) and the media was injected into the column after processing as described in the experimental section. Analytical conditions: 15 cm reversed-phase C18 column, flow rate 1 mL min^{-1}, column temperature 25 °C, injection volume 10 μL, mobile phase 20% H_2O—80% acetonitrile, both with a 0.1% trifluoroacetic acid. Fluorescence detector, excitation at 465 nm and emission at 530 nm. Percentages (mean ±SD, $n=3$) of the different metabolites, calculated from the peak areas, are: dihydroceramide (DHCer), 66±0.14; ceramide (Cer), 3±0.05; dihydroceramide-1-phosphate (DHCerP), 3±0.02; glucosyldihydroceramide (GlcDHCer), 8±0.01 and dihydrosphingomyelin (DHSM), 20±0.19. Calibration curves showed linear response in the concentration ranges of the analyses. *F*: Fluorescence; au: arbitrary units.

Inhibition of dihydroceramide desaturase by XM462

Using rat liver microsomes and a substrate concentration of 10 μM, desaturation of DHCerC6NBD was inhibited by XM462 and this inhibition was dose-dependent with an IC_{50} value of 8.2 μM. Incubations with different amounts of XM462 at varied substrate concentrations revealed that XM462 was a mixed-type inhibitor, with $K_i$app and α values of 2 μM and 0.83, respectively (Figure 2).

Desaturation of DHCerC6NBD was also inhibited by XM462 in intact Jurkat cells. As illustrated in Figure 3, a dose-dependent decrease of dihydroceramide desaturase activity was observed in the presence of 0.05 to 2 μM XM462. On the basis of these data, an IC_{50} value of 0.43 μM was calculated.

To confirm the dihydroceramide desaturase inhibitory activity of XM462, the amounts of natural ceramides and dihydroceramides present in cells after treatment with 5 μM XM462, a concentration that caused complete inhibition of DHCerC6NBD desaturation, were analysed by LC-MS. The results obtained are summarised in Figure 4. The *N*-palmitoyl and *N*-tetracosanoylamides were the main ceramide/dihydroceramide species.

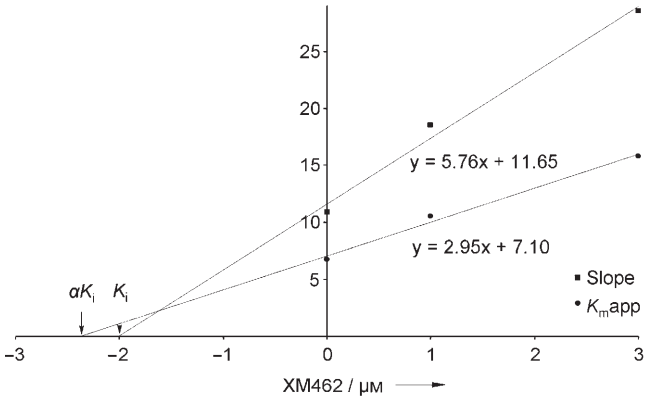

Figure 2. Type of inhibition of dihydroceramide desaturase by XM462. Inhibitory effect was investigated in rat liver microsomes, which were incubated with different amounts of XM462 at different substrate concentrations for one hour. The experiments were performed as described in the Experimental Section. Regression lines arise from data obtained in two different experiments with triplicates.

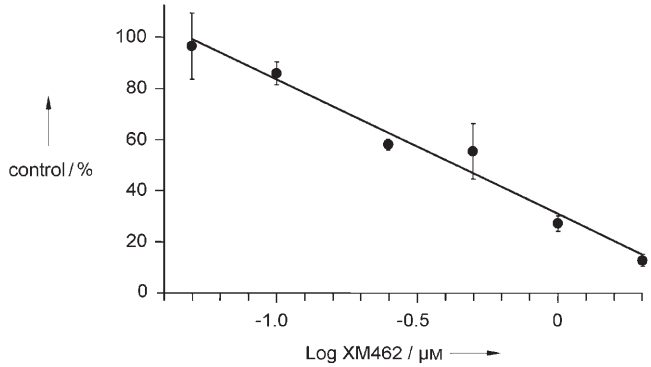

Figure 3. Concentration-dependence of dihydroceramide desaturase inhibition by XM462 in Jurkat A3 cells. Enzyme activity was determined as indicated in the experimental section using a substrate concentration of 10 μM and different concentrations of XM462 (0.05, 0.1, 0.25, 0.5, 1 and 2 μM). Data correspond to the mean ±SD of a representative experiment with three replicates. The calculated IC_{50} value is 0.43 μM (line equation: $y = 30.9–52.5x$; $R^2 = 0.97$)

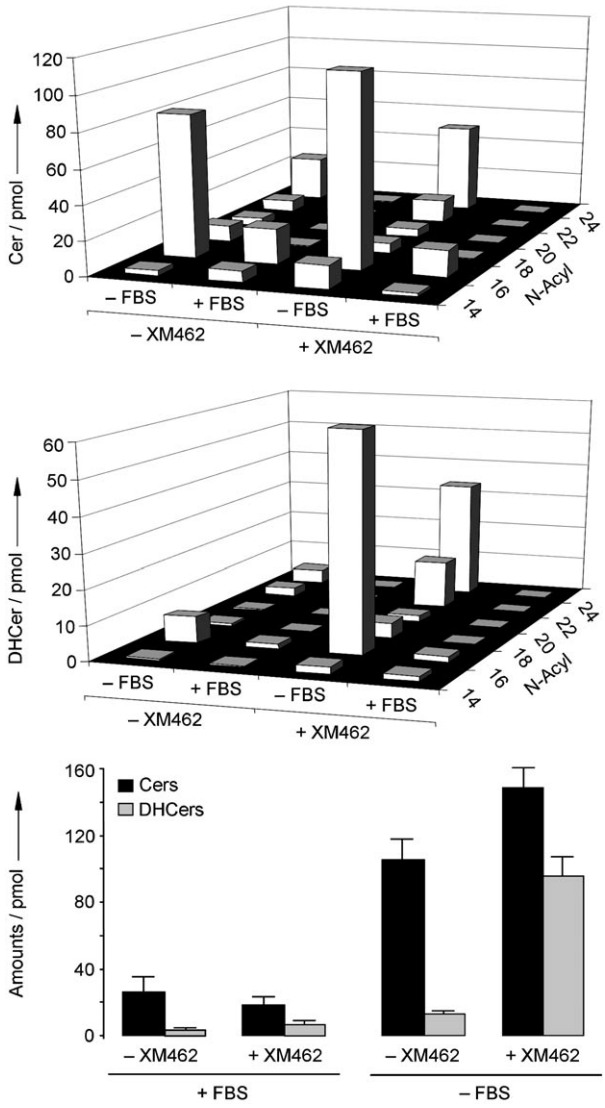

Figure 4. Effect of treatment with XM462 on production of natural ceramides and dihydroceramides. Analyses were conducted by LC-MS in extracts of jurkat cells treated with or without XM462 (5 μM, 24 h) in the presence or absence of FCS. Quantification was performed by comparison of areas with that of a known amount of *N*-dodecylsphingosine added as internal standard. Results are means ±SD of two independent analyses and are normalized with respect to the number of cells extracted. Cer, ceramides; DHCer, dihydroceramides.

Inhibition of the desaturase by XM462 was not evident when cells were cultured in the standard conditions (in the presence of serum). To stimulate sphingolipid metabolism beyond a basal level, the experiments were attempted in serum-free medium. In this case, amounts of ceramides increased to similar levels in both controls and XM462-treated cells as compared to cells cultured with serum. However, the amount of total dihydroceramides in XM462 treated cells were sixfold greater than those of controls. The ceramide/dihydroceramide ratios were 7 and 1.7 in vehicle and XM462 treated cells, respectively.

Metabolism of XM462

The same extracts used to determine mass ceramides/dihydroceramides were analysed for the presence of XM462 metabolites. As shown in Figure 5, the metabolites identified included the 1-phosphocholine (XM462-1PC, Figure 5 A e) and 1-glucosyl derivatives (Glc-XM462, Figure 5 A d), as well as the *N*-deacylation product (XM462-NH_2, Figure 5 A c) and its *N*-palmitoyl (XM462-NC16, Figure 5 A b) and *N*-stearoyl (XM462-NC18, Figure 5 A a) amides. Metabolism was higher in cells treated with XM462 in serum-free medium than in the presence of serum (Table 1).

Incubation of XM462 (5 and 10 μM) with rat liver microsomes in the same conditions used to determine the desaturase activity and further LC-MS analysis of methanolysed extracts showed the production of the phosphorylcholine derivative as the only metabolic product (mean ±SD percentage of XM462-PC versus XM462: 5 μM, 8.0±0.4; 10 μM, 10.2±0.2 ($n = 2$)).

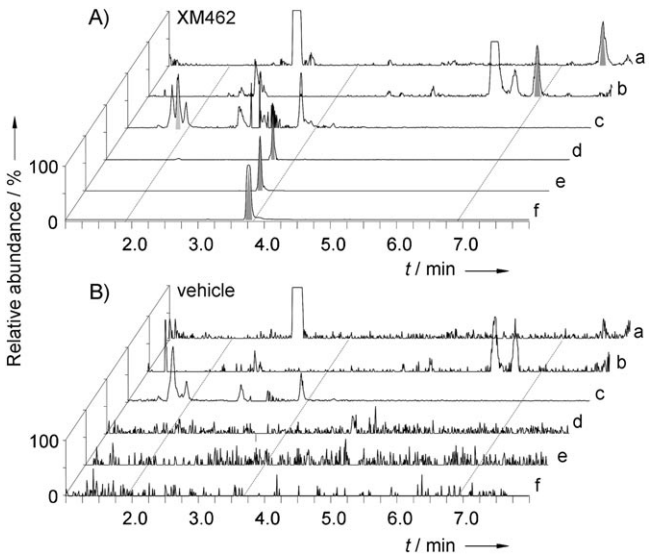

Figure 5. Metabolism of XM462 in Jurkat A3 cells. Selected ion chromatograms generated by LC-MS of a base methanolysed lipid extract of cells incubated with XM462 (5 μM) or vehicle (controls) in the absence of serum for 24 h (see experimental section for details). Traces correspond to: a, XM462-NC18; b, XM462-NC16; c, XM462-NH2; d, GlcXM462; e, XM462-1PC; f, XM462. In each trace, the peaks corresponding to XM462 metabolites are filled in grey Assignment details and the percentage of each metabolite with respect to the XM462 present in the extracts are given in Table 1. Metabolite structures and abbreviations are shown in Scheme 2.

Table 1. MS-Based assignments of XM462 metabolites present in extracts of Jurkat A3 cells.

Assignment[a]	Measured *m/z*	Theoretical *m/z*	error [ppm]	Molecular formula	−FBS/+FBS [%] [b]
XM462	446.3644	446.3668	−2.4	$C_{25}H_{51}NO_3S$	89.1/98.5
XM462-NH2	320.2609	320.2623	−1.4	$C_{17}H_{37}NO_2S$	0.9/n.d.
XM462-NC16	558.4916	558.4920	−0.4	$C_{33}H_{67}NO_3S$	0.22/n.d.
XM462-NC18	586.5268	586.5233	+ 3.5	$C_{35}H_{71}NO_3S$	0.18/n.d.
GlcXM462	608.4212	608.4196	+ 1.6	$C_{31}H_{61}NO_8S$	0.4/0.05
XM462-1PC	611.4195	611.4223	−2.8	$C_{30}H_{64}N_2O_6PS$	9.2/1.45

[a] Compound structures are shown in Scheme 2. [b] The amounts (pmol) of XM462, as calculated with reference to *N*-dodecylsphingosine as IS, was 590±62 (serum free medium) and 410±29 (serum added). Data was obtained from two replicates.

Cell viability

The effect of XM462 on cell viability was determined by the trypan blue exclusion assay. The percentage of unstained cells was significantly lower after treatment with XM462 (5 μM, 24 h) in the absence of serum (mean ±SD: 66±5.4, $n=4$; $p \leq 0.01$, unpaired two-tail t-test) than in the other cell populations, in which the percentage of trypan blue-negative cells was almost 100% (mean ±SD: vehicle/+FBS: 93±2.6; vehicle/-FBS 98±0.6; XM462/+FBS, 99±1.2, $n=4$).

Discussion

Emerging evidence indicate that dihydroceramides, the presumed inactive precursors of bioactive ceramides, are biologically active lipids.[9–11] In the studies carried out so far, it appears that the key to cytotoxicity of the chemotherapeutic drug fenretinide[9,11] and the cancer chemopreventive activity of γ-tocopherol[12] lie in their capacity to increase the intracellular levels of dihydroceramide, probably through inhibition of dihydroceramide desaturase activity. These reports underscore the potential usefulness of well characterised dihydroceramide desaturase inhibitors both in basic research studies as tools to decipher the role of dihydroceramides in cell biology and in cancer therapy. Following the rational design approach, a distinct modification of the dihydroceramide backbone has led to a new dihydroceramide desaturase inhibitor. Compound XM462 was conceived taking into account previous reports on the activity of some thiafatty acids as fatty acyl-CoA desaturase inhibitors. In *Saccharomyces cerevisiae*, for instance, 5-, 6-, 7-, 12-, and 13-thiastearic acids are converted into the respective Δ^9 desaturation products, whereas the analogues with sulfur in 8, 9, 10, or 11 block desaturation.[19] It was also shown that 9- and 10-thiastearic acid were strong inhibitors of the Δ^9 stearoyl-CoA desaturase in 7800 C1 Morris hepatoma cells, rat hepatocytes, and microsomes from rat liver.[20] On the other hand, thiafatty acids have also been used to inhibit leukotriene[21–23] and sterol[24] biosynthesis.

In light of these overall reports and the cryptoregiochemistry of dihydroceramide desaturase,[25] we anticipated that, as discussed below, a 5-thiadihydroceramide might inhibit this enzyme's activity.

Inhibition of dihydroceramide desaturase, probably the Des1 form, activity by XM462 was demonstrated both in vitro (rat liver microsomes) and in intact cells using DHCerC6NBD as the enzyme substrate. This fluorescent compound had been utilized by Kok et al.[18] to characterise the intracellular transport and metabolism of dihydroceramide in a number of different cell lines. The authors found that, amongst other metabolites, DHCerC6NBD was desaturated to the ceramide analogue, which suggested that this compound could be an appropriate substrate to measure dihydroceramide desaturase activity in vitro. As expected, we show that DHCerC6NBD is transformed into CerC6NBD in rat liver microsomes with K_m and V_{max} values of 7.7 μM and 19.3 pmol h^{-} mg^{-1}, respectively. XM462 inhibited this transformation with an IC_{50} value of 8.2 μM. This compound is less potent than GT11, which inhibits the desaturation of DHCerC6NBD with an observed IC_{50} value of 0.3 μM. Although this value is almost 100 times lower than that previously reported (20 μM),[13] this apparent discrepancy is explained considering that *N*-octanoylsphinganine was used as substrate in that first report. Kinetic experiments showed that XM462 produced a mixed-type inhibition with an apparent K_i in the low μM range. Similarly, 10-thiastearoyl-acyl carrier protein (ACP) was reported as a mixed-type inhibitor of the soluble Δ^9stearoyl-ACP desaturase complex.[26]

Inhibition of dihydroceramide desaturase by XM462 did also occur in Jurkat cells. In agreement with results found in HT29, NRK, BHK, or HL-60 cells,[18] experiments with DHCerC6NBD showed that this precursor was metabolised to dihydrosphingomyelin, glucosyldihydroceramide, and dihydroceramide-1-phosphate. Besides these three compounds, which accounted for approximately 30% of the total metabolites, CerC6NBD was also detected. CerC6NBD amounts decreased in the presence of XM462 in a dose-dependent manner, with an IC_{50} value of 0.43 μM. In the same experimental conditions, GT11 inhibited the formation of unsaturated sphingolipids from DHCerC6NBD in Jurkat A3 cells with an IC_{50} value of 55 nM. This value is similar to that previously reported (23 nM) in primary cultured neurons and radioactive *N*-octanoylsphinganine as substrate.[16] However, the lower in vitro potency of XM462 compared with GT11 in intact cells is widely counterbalanced by its simpler synthesis and higher chemical stability. Furthermore, it is conceivable that ongoing chemical modifications of the XM462 core structure will lead to more potent analogues.

Although the mechanism of inhibition has not been investigated, we anticipated that XM462 would behave as a substrate mimic therefore binding to the enzyme active site. Transformation of dihydroceramide into ceramide by dihydroceramide desaturase occurs in two steps, the rate-limiting abstraction of the *pro*-(*R*) C4-H followed by fast elimination of the *pro*-(*S*) C5-H.[25] According to this mechanism, XM462 would afford the intermediate carbon centred radical species **1**, in equilibrium with the sulfur centred radical **2**. The inhibition may then arise from coordination of the intermediate(s) to the enzyme oxidant (probably a hypervalent diirondioxo complex) or interaction with the disulfide bond(s) proposed to be required for catalytic activity.[27] A few studies using the soluble acyl-ACP Δ^9 desaturase have shown that when the desaturase oxidant is not optimally aligned with the heteroatom of a thia- or oxa-substrate analogue, a chain-cleavage process can occur[26,28] and enzyme inhibition may be elicited by one of the cleavage products. The analysis of XM462 metabolites indicated that this compound is hydrolysed and reacylated and that it is also metabolised to the 1-glucosyl and 1-phosphocholine derivatives (Scheme 2, Table 1). Des1-catalyzed cleavage products **3a** and **4** (Scheme 3), similar to those reported with 9-thiastearoyl-ACP and the soluble acyl-ACP Δ^9 desaturase, were not found in this study after incubation with either intact cells (Scheme 2, Table 1) or rat liver microsomes. Likewise, the putative oxidation products **3b** and tridecyldisulfide have not been detected. Therefore, it does not appear that a product of the Des1-catalysed inhibitor cleavage causes inhibition.

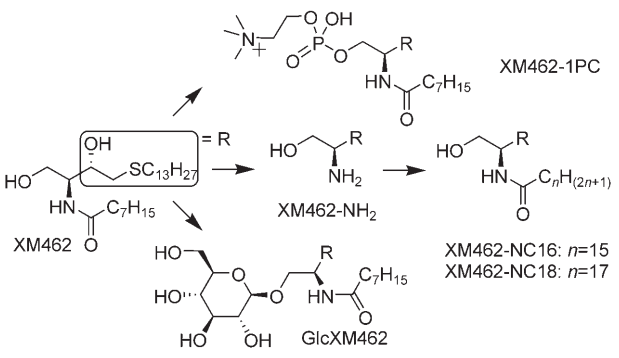

Scheme 2. Metabolism of XM462.

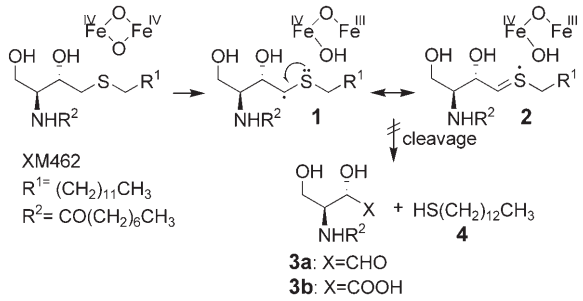

Scheme 3. Structure of XM462 and putative Des1-catalysed oxidation and cleavage species.

As expected from its dihydroceramide desaturase inhibitory activity, XM462 brought about an accumulation of natural dihydroceramides, which became evident if cells were stressed by culture in serum-deprived medium. Under the same conditions, ceramides built up not only in controls, as expected, but also in XM462-treated cells. In agreement with the results reported by Separovic et al. in Jurkat cells,[29] the *N*-hexadecanoyl and, to a lesser extent, the *N*-tetracosanoyl species were the most abundant amongst the different *N*-acyl groups. Accumulation of C16 ceramide preceding cell-cycle arrest and further apoptosis has also been reported in LNCaP prostate cancer cells following androgen ablation,[30,31] and in Jurkat T-cells after either irradiation or Fas cross-linking.[32] An increase in C16 and C24 ceramides during apoptosis of dendritic cells induced by tumour culture supernatant has also been described.[33] The increase of ceramides observed in XM462-treated cells may indicate that not only the de novo pathway, but also the sphingomyelinase activity contribute to the generation of ceramide in cells cultured in serum-free medium. As total ceramide mass in cells is much lower than that of sphingomyelin (approximately 8% in the Jurkat cells used in this study), the contribution of sphingomyelin hydrolysis to ceramide increase could not be demonstrated by UPLC-TOF analysis.

The effect of serum withdrawal on ceramide production and cell death has been extensively reported in the literature. In general, serum withdrawal causes an increase in ceramide levels accompanied with induction of the apoptotic pathway.[34–39] The ceramide rise does usually result from activation of a sphingomyelinase[35,36,39] or the de novo pathway.[40] However, Jurkat cell viability, as the percentage of trypan blue unstained cells in total cells, was not significantly affected after incubation in serum deprived medium for 24 h, although it decreased in the same conditions upon XM462 treatment. These results seem to indicate that dihydroceramides, but not ceramides, may mediate the sensitivity of the Jurkat A3 cells to serum withdrawal. In this regard, Turnbull et al.[41] reported that daunorubicin-induced apoptosis does not appear to be mediated by ceramide in the lymphoblastic leukaemia cell line Jurkat E6-1. Likewise, in the same cell line the levels of ceram-

ides and dihydroceramides are increased in response to photodamage, but only dihydroceramides respond in a dose-dependent way. This result suggests that dihydroceramides may play a role in photodamage-induced cell death. In a recent article, using both pharmacological and genetic tools, Kraveka et al.[9] demonstrated that the partial loss of Des1 activity in human neuroblastoma cells inhibited cell growth with cell cycle arrest at G_0/G_1 and a significant hypophosphorylation of retinoblastoma protein. Furthermore, it was also shown that this effect was paralleled by an increase in dihydroceramides, but not ceramides, in cells. On the other hand, Zheng et al.[11] have reported that dihydroceramides induce autophagy and may be important in the regulation of this important cellular process. These overall results emphasise that dihydroceramides may be of importance in cancer biology. The mechanism involved in the cytotoxicity of XM462 observed upon serum removal and other stress stimuli will be investigated in the near future.

Conclusions

Rational design has led to the discovery of the 5-thiadihydroceramide XM462 as a new dihydroceramide desaturase inhibitor. Although this compound is less potent than GT11 in the systems investigated, it is more easily available by synthesis, more chemically stable, and quite resistant to metabolic transformation, which, in addition to its effectiveness both in vitro and in cultured cells, makes it a good candidate for future research aimed at deciphering the biological functions of dihydroceramides. Its capability of decreasing cell viability under stress suggests that it deserves further attention as a potential anticancer agent. Finally, as mice lacking Des1 are refractory to insulin resistance,[42] this compound may have potential to treat type 2 diabetes. Further studies along these lines are ongoing in our laboratories.

Experimental Section

Sphingolipids were from Avanti Polar Lipids. 6-(7-Nitrobenzofurazan-4-ylamino)hexanoic acid, 1-hydroxybenzotriazole (HOBT), *N*-Ethyl-*N*′-(3-dimethylaminopropyl)carbodiimide (EDC), bovine serum albumin (BSA), reduced nicotinamide adenine dinucleotide (NADH), trypan blue, penicillin/streptomycin (100 x solution), and cell-culture quality L-glutamine and sodium pyruvate were purchased from Sigma. Silica gel for flash chromatography was from Merck. HPLC quality trifluoroacetic acid and acetonitrile were used and all other solvents were of the highest purity available. RPMI 1640 media and foetal calf serum (FCS) were purchased from Gibco. ^{1}H NMR spectra were recorded in $CDCl_3$ using a Varian Unity 300 instrument. IR spectra were recorded with a Bomem Michelson MB-120 instrument. High-resolution mass spectra (HRMS) were obtained with a Waters Micromass LCT Premier apparatus equipped with a dual electrospray (ESI) LockSpray ion source and data were acquired in positive ESI. Both DHCerC6NBD and XM462 were stored dry at −20 °C protected from light. Stock solutions (2 to 4 mM in ethanol) for biochemical experiments were kept at −20 °C in glass vials.

Synthesis of compounds

DHCer-C6NBD. A mixture of 6-(7-nitrobenzofurazan-4-ylamino)hexanoic acid (9.7 mg, 0.033 mmol), EDC (6.1 mg, 0.036 mmol), and HOBT (5.0 mg, 0.033 mmol) was dissolved in CH_2Cl_2 (50 mL mmol^{-1}) and stirred for 20 min. The resulting mixture was added over a solution of sphinganine (10 mg, 0.033 mmol) in CH_2Cl_2 (35 mL mmol^{-1}). After stirring for 16 h at RT, water (20 mL) was added and the product was extracted with CH_2Cl_2. The combined organic layers were dried over $MgSO_4$, the salt was filtered off, and the solvent was removed under reduced pressure to give DHCer-C6NBD (13.7 mg, 0.023 mmol, 72%) as a reddish solid after purification by flash chromatography (CH_2Cl_2:MeOH 97:3). ^{1}H NMR: $\delta =$ 0.87 (t, 3H, CH_3), 1.29 (s, 28H, 14xCH_2 aliphatic), 1.55 (m, 2H), 1.76 (m, 2H), 1.84 (m, 2H), 2.31 (t, $J = 6.3$ Hz, 2H, CH_2CONH), 3.06 (bs, 2H, CH_2NH-Ar), 3.78 (dd, $J = 3.5$ and 11.5 Hz, 1H, C(1)H), 3.80 (m, 1H, C(2)H), 3.89 (m, 1H, C(3)H), 4.05 (dd, $J = 3.5$ and 11.5 Hz, C(1)H′), 6.17 (d, $J = 8.7$ Hz, A part of an AB system, 1H), 6.43 (d, $J =$ 8.7 Hz, B part of an AB system, 1H), 6,68 (bs, 1H, NH), 8,49 ppm (d, $J = 8.7$ Hz, 1H, CONH). HRMS calcd for $C_{30}H_{51}N_5O_6$: 577.3839; found: 577.3837.

(S, 1′S)-tert-butyl 4-(1-hydroxy-2-(tridecylthio)ethyl)-2,2-dimethyloxazolidine-3-carboxylate (2). Sodium hydride (100 mg of a 60% dispersion in mineral oil, equivalent to 2.5 mmol) was placed in a three-necked flask and thoroughly washed under Ar with 3×5 mL of hexanes. To the resulting solid, DMF (5 mL) was added by syringe and the resulting suspension cooled to 5 °C (ice-water bath). A solution of tridecane-1-thiol (500 mg, 2.3 mmol) in DMF (5 mL) was then slowly added dropwise by syringe. When the reaction was complete, as evidenced by the absence of gas evolution, a solution of epoxide 1[17] (370 mg, 1.5 mmol) in DMF (5 mL) was added dropwise and the reaction mixture was next stirred at 40 °C. After 4 h, the mixture was cooled and treated with 1N HCl (25 mL), extracted with 3×15 mL of Et_2O, dried, and evaporated. The resulting crude was flash-chromatographed on hexanes/EtOAc (8:1) to afford **2** (654 mg, 1.42 mmol, 95%). ^{1}H NMR (500 MHz): $\delta = 0.83$ (t, 3H, $J = 6.6$ Hz, CH_3 aliphatic), 1.2–1.25 (broad, 18H, 9 x CH_2 aliphatic), 1.3–1.35 (m, 2H, CH_2 aliphatic), 1.35 (s, 6H, 2 x CH_3 oxazolidine), 1.4 (s, 9H, 3 x CH_3, *tert*-butyl), 1.5–1.6 (m, 2H, CH_2 aliphatic), 2.4–2.6 (m, 3H, C(H′)S + CH_2(S)), 2.6 (dd, 1H, $J = 13.6$ Hz, $J' = 3.1$ Hz, C(H)S), 3.1 (broad, 1H, OH), 3.7–3.8 (m, 1H, CH (N cycle)), 3.8–4.1 ppm (m, 3H, CHH′(O cycle) + CH-hydroxyl) (mixture of rotamers). ^{13}C NMR (125 MHz): $\delta = 14.1$, 22.7, 23.1, 24.4, 26.9, 27.6, (28.5, 28.8), (29.2, 29.3), (29.5, 29.6), (29.7, 30.0), (31.6, 31.9), 32.3, 33.8, 34.5 ppm, (57.2, 57.3) (C4), (66.2, 66.5) (C5), (71.0, 71,2) (C1′) (79.8, 80.2) (C-O-*t*Bu), (93.7, 94.2) (C2), (151.4, 152.0) (COO*t*Bu) (mixture of rotamers). $[\alpha]_D = +$ 0.87 ($c = 0.5$, $CHCl_3$, 20 °C).

(2S, 3S)-2-amino-4-(tridecylthio)butane-1,3-diol (3). A solution of **2** (600 mg, 1.31 mmol) in CH_2Cl_2 (10 mL) was treated with TFA (1 mL) and stirred at RT for 20 min. The reaction mixture was next evaporated to dryness, taken up in CH_2Cl_2 (10 mL), and washed with 1N NaOH solution (5 mL) and water. The organic phase was dried and evaporated to give **3** (418 mg, 1.31 mmol, quantitative). IR (NaCl): 3348, 2917, 2853, 1464, 1050, 717 cm^{-1}. ^{1}H NMR (500 MHz, $CDCl_3$): $\delta = 0.85$ (t, 3H, $J = J' = 6.7$ Hz, CH_3), 1.2–1.3 (m, 18H, 9 x CH_2 aliphatic), 1.3–1.4 (m, 2H, CH_2 aliphatic), 1.56 (m, 2H, CH_2 aliphatic), 2.5 (t, 2H, $J = J' = 7.5$ Hz, C(6)H), 2.6 (dd, 1H, $J =$ 13.2 Hz, $J' = 8.7$ Hz, C(4)H), 2.6 (broad, 3H), 2.8 (dd, 1H, $J = 13.2$ Hz, $J' = 3.7$ Hz, C(4)H′), 2.9 (broad, 1H, C(2)H), 3.6–3,8 ppm (m, 3H, $C(1)H_2 + C(3)H$). ^{13}C NMR (125 MHz, $CDCl_3$): $\delta = 14.1$, 22.7, 28.8, 29.2, 29.3, 29.5, 29.6, 29.6, 29.7, 31.9 (C7), 32.2 (C6), 36.7 (C4), 55.4 (C2), 63.9 (C1), 72.0 ppm (C3). $[\alpha]_D = +$ 7.3 ($c = 1.0$, $CHCl_3$, 20 °C). HRMS calcd for $C_{17}H_{37}NO_2S$: 319.2545; found: 319.2532.

(2′S,3′S)-N-[1,3-dihydroxy-4-(tridecylthio)but-2-yl]octanamide (XM462). A solution of octanoyl chloride (223 mg, 1.4 mmol) in THF (3 mL) is added dropwise over a solution of **3** (400 mg, 1.25 mmol) in 10 mL of a 1:1 mixture of aqueous 50% NaOAc in THF. The reaction mixture is vigorously stirred at RT for 8 h, concentrated under reduced pressure, diluted with H_2O (20 mL), and extracted with CH_2Cl_2. The organic extract is dried, evaporated, and the residue is purified by flash chromatography (CH_2Cl_2/MeOH, 97:3) to afford XM462 (470 mg, 1.05 mmol, 85%). IR (NaCl): 3295 (OH), 2923, 2853, 1638 (amide), 1548, 1463, 1068, 717 cm^{-1}. ^1H NMR (500 MHz, $CDCl_3$): $\delta = 0.85$ (t, 6H, $J = J' = 6.9$ Hz, 2 x CH_3 aliphatic), 1.2–1.3 (m, 28H, 14 x CH_2 aliphatic), 1.53 (dd, 2H, $J =$ 7.6 Hz, $J' = 2.5$ Hz, C(7′)H), 1.6 (m, 2H, C(3)H), 2.2 (t, 2H, $J = J' =$ 7.6 Hz, C(2)H), 2.5 (t, 2H, $J = J' = 7.2$ Hz, C(6′)H), 2.55–2.65 (m, 1H, C(4′)H), 2.7–2.8 (m, 1H, C(4′)H′), 3.1 (broad, 2H), 3.6 (dd, 1H, $J =$ 11.4 Hz, $J' = 3.4$ Hz, C(1′)H), 3.8 (dt, 1H, $J = 11.4$ Hz, $J' = 4.0$ Hz, C(1′)H′), 3.9 (dt, 1H, $J = 7.6$ Hz, $J' = 3.7$ Hz, C(2′)H), 4.0 (dd, 1H, $J =$ 9.0 Hz, $J' = 3.2$ Hz, C(3′)H), 6.4 ppm (d, 1H, $J = 8.0$ Hz, CONH). ^{13}C NMR (125 MHz, $CDCl_3$): $\delta = 14.0$–14.1 (C8 and C18′), 22.6–22.7 (C7 and C17′), 25.7 (C3), 28.8–29.7 (C4, C5, C8′ to C15′), 31.7–32.1 (C6, C7′, C16′), 36.8 (C2), 53.4 (C2′), 61.9 (C1′), 71.2 (C3′), 173.8 (CO). $[\alpha]_D = +$ 0.8 ($c = 1.0$, $CHCl_3$, 20 °C) HRMS calcd for $C_{25}H_{52}NO_3S$: 446.3668; found: 446.3649.

Biological activity

Preparation of rat liver microsomes. Microsomes were prepared from livers of 200–250 g female Sprague-Dawley rats euthanised by decapitation. The livers were excised and washed twice in ice-cold sucrose/phosphate buffer (0.25 M sucrose, 100 mM NaH_2PO_4/Na_2HPO_4, pH 7.4), after which they were weighed and chopped up using a scalpel. Then the minced livers were added to the same sucrose/phosphate buffer (0.5 g liver mL^{-1}) and homogenised with five up-and-down strokes at 600 rpm using a Braun glass homogeniser fitted with a Teflon pestle. The resulting homogenate was spun down at 680 x *g* for 10 min. The supernatant was saved while the pellet was resuspended and span down again under the same conditions described above. The combined supernatants were centrifuged at 105,000 x *g* for 1 h. The resulting pellet was resuspended in phosphate buffer (100 mM NaH_2PO_4/Na_2HPO_4, pH 7.4), the microsome protein content determined by the Bradford assay, and stored at −80 °C.

Cell culture. Jurkat A3, a human immortalised lymphocytic cell line, was cultured at 37 °C according to standard cell culture methods using RPMI 1640 media supplemented with 2 mM L-glutamine, 1 mM sodium pyruvate, 10% foetal calf serum, penicillin, and streptomycin. Cells were seeded at 0.2×10^6 cells mL^{-1} and passaged at a cell density of 0.8×10^6 cells mL^{-1}.

Dihydroceramide desaturase activity in rat liver microsomes. The substrate was first added to an eppendorf tube and evaporated under a stream of N_2 gas. If necessary, inhibitors were also added at this point. The substrate or substrate/inhibitor solids were dissolved in 10 μL ethanol and complemented with 80 μL of a 10 mg mL^{-1} BSA/PB solution. The mixture was sonicated for 3 min. A total of 0.3 mg of protein was added from the microsomal suspension together with 30 μL of a 33 mM NADH/PB solution. The reaction volume was then made up to 300 μL and samples were incubated at 37 °C for 1 h. To stop the reaction, 800 μL of methanol was added to each tube and the resulting supernatant was kept at 4 °C overnight to allow a white precipitate to form. Finally, the samples were spun down in a tabletop microfuge at 14000 rpm for 3 min. HPLC coupled to a fluorescence detector was used to measure the dihydroceramide desaturase activity by injecting 14 μL of the supernatant.

Dihydroceramide desaturase activity in Jurkat A3 cells. Jurkat A3 cells were grown and seeded at 10^6 cells mL^{-1} in a 24-well tissue culture plate (400 μL $well^{-}$). The required amount of substrate was evaporated under a steam of N_2 to minimise the amount of ethanol added to the cells. For a single-well assay, 2 μL of ethanol was added to the substrate solid and supplemented with 100 μL of cell culture media. The substrate/media mixture was then supplied to the well, and the cells were incubated at 4 °C for 30 min to allow substrate uptake into the cells. After the cold incubation, the cell suspension was spun down at 1300 rpm for 3 min. The cell pellet was resuspended in 400 μL of fresh media. At this point, the inhibitors were added to the cells if needed to be. The assay incubation time was 3 h at 37 °C/5% CO_2. Upon completion, the content of each well were transferred to 1.5 mL eppendorf tube and centrifuged in a tabletop microfuge at 14,000 rpm for 3 min. Both the resulting supernatant and pellets were kept. In the first place, the roughly 400 μL of supernatant were complemented with 600 μL methanol and centrifuged at 14,000 rpm for 3 min. The supernatant was transferred to HPLC vials and the pellet, if present at all, was discarded. Secondly, the cell pellet was resuspended in 100 μL H_2O and sonicated for 30 seconds. To the resulting cell lysate, 900 μL methanol were added, and centrifuged at 14,000 rpm for 3 min. The supernatant was transferred to HPLC vials. Both the cell lysate and supernatant samples were analysed by HPLC coupled to a fluorescence detector. A total of 100 μL was injected from the lysate fraction, whereas only 25 μL was analysed in the case of the cell media fraction.

HPLC-FD analysis. All HPLC analyses were performed with an Alliance apparatus coupled to a fluorescence detector using a reversed-phase column eluted with 20% H_2O and 80% acetonitrile, both with a 0.1% of trifluoroacetic acid, flowing at 1 mL mL^{-1}. The detector was set at an excitation wavelength of 465 nm and measure the emission wavelength at 530 nm. Each sample was run for up to 15 min.

Effect of XM462 on natural ceramide and dihydroceramide production. Jurkat A3 cells were harvested and seeded at a cell density of 0.8×106 cells mL^{-1} in 10 mL of the appropriate RPMI 1640 media supplemented with 10% foetal bovine serum. In parallel, cells were also prepared in the absence of serum. Cells were treated with the inhibitor and incubated for 24 h at 37 °C, 5% CO_2. After the incubation, cell survival was assessed microscopically using trypan blue. Cells were pelleted, washed in PBS, and transferred to glass vials. Sphingolipid extracts, fortified with internal standards (*N*-dodecanoylsphingosine, *N*-dodecanoylglucosylsphingosine, and *N*-dodecanoylsphingosylphosphorylcholine, 0.5 nmol each), were prepared as described[43] and analysed. The liquid chromatography-mass spectrometer consisted of a Waters Aquity UPLC system connected to a Waters LCT Premier orthogonal accelerated time of flight mass spectrometer (Waters, Millford, MA), operated in positive electrospray ionisation mode. Full scan spectra from 50 to 1500 Da were acquired and individual spectra were summed to produce data points each 0.2 s. Mass accuracy and reproducibility were maintained by using an independent reference spray by the LockSpray interference. The analytical column was a 100 mm × 2.1 mm i.d., 1.7 μm C8 Acquity UPLC BEH (Waters). The two mobile phases were phase A: methanol/water/formic acid (74/25/1 *v/v/v*); phase B: methanol/formic acid (99/1 *v/v*), both also contained 5 mM ammonium formate. A linear gradient was programmed—0.0 min: 80% B; 3 min: 90% B; 6 min: 90% B; 15 min: 99% B; 18 min: 99% B; 20 min: 80% B. The flow rate was 0.3 mL min^{-1}. The column was held at 30 °C. Quantification was carried out using the extracted ion chromatogram of each compound, using 50 mDa

windows. The linear dynamic range was determined by injecting standard mixtures. Positive identification of compounds was based on the accurate mass measurement with an error <5 ppm and its LC retention time, compared to that of a standard ($\pm 2\%$). The identification of XM462 metabolites was performed in the same samples, using the extracted ion chromatogram of the expected compound, using a 50 mDa window, and were confirmed by checking that the accurate mass measurement had an error <5 ppm.

Trypan blue staining. 24 h post treatment, cells (50 μL) were diluted 1:1 with trypan blue (0.4% in PBS) and counted using a haemocytometer chamber. At least 200 cells were counted for each data point. The means and SDs were calculated from three independent determinations.

Acknowledgements

This work was funded by the Spanish Council for Scientific Research (CSIC, Grant 200580F0211), Fundación para la Investigación y Prevención del SIDA en España (FIPSE, Grant 36550/06), Generalitat de Catalunya (Grant 2005SGR05-01063) and Ministerio de Educación y Ciencia (Grant CTQ2005-00175/BQU). We thank Dr. D. Canals for determining the LC-MS linear dynamic ranges used in this study.

Keywords: ceramide · enzyme inhibitors · lipids · MS · thiasphinganine

[1] K. Endo, T. Akiyama, S. Kobayashi, M. Okada, *Mol. Gen. Genet.* **1996**, *253*, 157–165.
[2] K. Endo, Y. Matsuda, S. Kobayashi, *Dev. Growth Differ.* **1997**, *39*, 399–403.
[3] P. Ternes, S. Franke, U. Zahringer, P. Sperling, E. Heinz, *J. Biol. Chem.* **2002**, *277*, 25512–25518.
[4] F. Omae, M. Miyazaki, A. Enomoto, M. Suzuki, Y. Suzuki, A. Suzuki, *Biochem. J.* **2004**, *379*, 687–695.
[5] F. Omae, M. Miyazaki, A. Enomoto, A. Suzuki, *FEBS Lett.* **2004**, *576*, 63–67.
[6] A. Bielawska, H. M. Crane, D. Liotta, L. M. Obeid, Y. A. Hannun, *J. Biol. Chem.* **1993**, *268*, 26226–26232.
[7] E. H. Ahn, J. J. Schroeder, *Exp. Biol. Med.* **2002**, *227*, 345–353.
[8] H. Sugiki, Y. Hozumi, H. Maeshima, Y. Katagata, Y. Mitsuhashi, S. Kondo, *Br. J. Dermatol.* **2000**, *143*, 1154–1163.
[9] J. M. Kraveka, L. Li, Z. M. Szulc, J. Bielawski, B. Ogretmen, Y. A. Hannun, L. M. Obied, A. Bielawska, *J. Biol. Chem.* **2007**, *282*, 16718–16728.
[10] J. Stiban, D. Fistere, M. Colombini, *Apoptosis* **2006**, *11*, 773–780.
[11] W. Zheng, J. Kollmeyer, H. Symolon, A. Momin, E. Munter, E. Wang, S. Kelly, J. C. Allegood, Y. Liu, Q. Peng, H. Ramaraju, M. C. Sullards, M. Cabot, A. H. Merrill, *Biochim. Biophys. Acta Biomembr.* **2006**, *1758*, 1864–1884.
[12] Q. Jiang, J. Wong, H. Fyrst, J. D. Saba, B. N. Ames, *Proc. Natl. Acad. Sci. USA* **2004**, *101*, 17825–17830.
[13] G. Triola, G. Fabrias, A. Llebaria, *Angew. Chem.* **2001**, *113*, 2014–2016; *Angew. Chem. Int. Ed.* **2001**, *40*, 1960–1962.
[14] G. Triola, G. Fabrias, J. Casas, A. Llebaria, *J. Org. Chem.* **2003**, *68*, 9924–9932.
[15] C. Bedia, G. Triola, J. Casas, A. Llebaria, G. Fabrias, *Org. Biomol. Chem.* **2005**, *3*, 3707–3712.
[16] G. Triola, G. Fabrias, M. Dragusin, L. Niederhausen, R. Broere, A. Llebaria, G. Van Echten-Deckert, *Mol. Pharmacol.* **2004**, *66*, 1671–1678. .
[17] W. J. Moore, F. A. Luzzio, *Tetrahedron Lett.* **1995**, *36*, 6599–6602.
[18] J. W. Kok, M. Nikolova-Karakashian, K. Klappe, C. Alexander, A. H. Merrill, Jr., *J. Biol. Chem.* **1997**, *272*, 21128–21136.
[19] P. H. Buist, H. G. Dallmann, R. R. Rymerson, P. M. Seigel, P. Skala, *Tetrahedron Lett.* **1988**, *29*, 435–438.
[20] K. E. Høvik, Ø. S. Spydevold, J. Bremer, *Biochim. Biophys. Acta Lipids Lipid Metab.* **1997**, *1349*, 251–256.
[21] E. J. Corey, J. R. Cashman, T. M. Eckrich, C. D. R. , *J. Am. Chem. Soc.* **1985**, *107*, 713–715.
[22] M. O. Funk, A. W. Alteneder, *Biochem. Biophys. Res. Commun.* **1983**, *114*, 937–943.
[23] E. J. Corey, M. d'Alarcao, K. S. Kyler, *Tetrahedron Lett.* **1985**, *26*, 3919–3922.
[24] D. Stach, Y. F. Zheng, A. L. Perez, A. C. Oehlschlager, I. Abe, G. D. Prestwich, P. G. Hartman, *J. Med. Chem.* **1997**, *40*, 201–209.
[25] C. K. Savile, G. Fabrias, P. H. Buist, *J. Am. Chem. Soc.* **2001**, *123*, 4382–4385.
[26] R. D. White, B. G. Fox, *Biochemistry* **2003**, *42*, 7828–7835.
[27] C. Michel, G. van Echten-Deckert, J. Rother, K. Sandhoff, E. Wang, A. H. Merrill, Jr., *J. Biol. Chem.* **1997**, *272*, 22432–22437.
[28] C. E. Rogge, B. G. Fox, *Biochemistry* **2002**, *41*, 10141–10148.
[29] D. Separovic, K. Hanada, M. Y. Maitah, B. Nagy, I. Hang, M. A. Tainsky, J. M. Kraniak, J. Bielawski, *Biochem. Biophys. Res. Commun.* **2007**, *358*, 196–202.
[30] M. Eto, J. Bennouna, O. C. Hunter, P. A. Hershberger, T. Kanto, C. S. Johnson, M. T. Lotze, A. A. Amoscato, *Prostate* **2003**, *57*, 66–79.
[31] M. Eto, J. Bennouna, O. C. Hunter, M. T. Lotze, A. A. Amoscato, *Int. J. Urol.* **2006**, *13*, 148–156.
[32] R. L. Thomas, Jr., C. M. Matsko, M. T. Lotze, A. A. Amoscato, *J. Biol. Chem.* **1999**, *274*, 30580–30588.
[33] T. Kanto, P. Kalinski, O. C. Hunter, M. T. Lotze, A. A. Amoscato, *J. Immunol.* **2001**, *167*, 3773–3784.
[34] R. Caricchio, L. D'Adamio, P. L. Cohen, *Cell Death Differ.* **2002**, *9*, 574–580.
[35] D. J. Fernandez-Ayala, S. F. Martin, M. P. Barroso, C. Gomez-Diaz, J. M. Villalba, J. C. Rodriguez-Aguilera, G. Lopez-Lluch, P. Navas, *Antioxid. Redox Signaling* **2000**, *2*, 263–275.
[36] S. Jayadev, B. Liu, A. E. Bielawska, J. Y. Lee, F. Nazaire, M. Y. Pushkareva, L. M. Obeid, Y. A. Hannun, *J. Biol. Chem.* **1995**, *270*, 2047–2052.
[37] M. P. Muriel, N. Lambeng, F. Darios, P. P. Michel, E. C. Hirsch, Y. Agid, M. Ruberg, *J. Comp. Neurol.* **2000**, *426*, 297–315.
[38] D. Papineau, A. Gagnon, A. Sorisky, *Metabolism* **2003**, *52*, 987–992.
[39] M. E. Venable, J. Y. Lee, M. J. Smyth, A. Bielawska, L. M. Obeid, *J. Biol. Chem.* **1995**, *270*, 30701–30708.
[40] M. U. Yu, J. M. Yoo, Y. S. Lee, Y. M. Lee, J. T. Hong, K. W. Oh, S. Song, Y. P. Yun, H. S. Yoo, S. Oh, *J. Toxicol. Environ. Health Part A* **2004**, *23*, 2085–2094.
[41] K. J. Turnbull, B. L. Brown, P. R. M. Dobson, *Leukemia* **1999**, *13*, 1056–1061.
[42] W. L. Holland, J. T. Brozinick, L. P. Wang, E. D. Hawkins, K. M. Sargent, Y. Liu, K. Narra, K. L. Hoehn, T. A. Knotts, A. Siesky, D. H. Nelson, S. K. Karathanasis, G. K. Fontenot, M. J. Birnbaum, S. A. Summers, *Cell Metab.* **2007**, *5*, 167–179.
[43] A. H. Merrill, Jr., M. C. Sullards, J. C. Allegood, S. Kelly, E. Wang, *Methods* **2005**, *36*, 207–224.

Received: November 12, 2007
Revised: January 9, 2008
Published online on January 31, 2008

